Molecular Therapy
Methods & Clinical Development
Original Article

AAV2/9-mediated gene transfer into murine lacrimal gland leads to a long-term targeted tear film modification

Benoit Gautier,[1] Léna Meneux,[1] Nadège Feret,[1] Christine Audrain,[2] Laetitia Hudecek,[1,3] Alison Kuony,[1,4] Audrey Bourdon,[5] Caroline Le Guiner,[5] Véronique Blouin,[5] Cécile Delettre,[1] and Frédéric Michon[1]

[1]Institute for Neurosciences of Montpellier, University of Montpellier, INSERM, Montpellier, France; [2]TarGeT, Nantes University, INSERM UMR 1089, CHU Nantes, Nantes, France; [3]MRI, Biocampus, University of Montpellier, CNRS, INSERM, Montpellier, France; [4]Cell Adhesion and Mechanics Lab, Université de Paris, CNRS, Institut Jacques Monod, Paris, France; [5]INSERM UMR 1089, Université de Nantes, CHU de Nantes, Nantes, France

Corneal blindness is the fourth leading cause of blindness worldwide. Since corneal epithelium is constantly renewed, non-integrative gene transfer cannot be used to treat corneal diseases. In many of these diseases, the tear film is defective. Tears are a complex biological fluid secreted by the lacrimal apparatus. Their composition is modulated according to the context. After a corneal wound, the lacrimal gland secretes reflex tears, which contain growth factors supporting the wound healing process. In various pathological contexts, the tear composition can support neither corneal homeostasis nor wound healing. Here, we propose to use the lacrimal gland as bioreactor to produce and secrete specific factors supporting corneal physiology. In this study, we use an AAV2/9-mediated gene transfer to supplement the tear film. First, we demonstrate that a single injection of AAV2/9 is sufficient to transduce all epithelial cell types of the lacrimal gland efficiently and widely. Second, we detect no adverse effect after AAV2/9-mediated nerve growth factor expression in the lacrimal gland. Only a transitory increase in tear flow is measured. Remarkably, AAV2/9 induces an important and long-lasting secretion of this growth factor in the tear film. Altogether, our findings provide a new clinically applicable approach to tackle corneal blindness.

INTRODUCTION

To ensure clear vision, the anterior parts of the eye, namely the cornea and lens, need to be fully transparent. While the lens is protected by being located inside the eye, the cornea is the most external tissue of the eye, and thus prone to environmental aggressions. This ectodermal organ is subjected to lifelong cell renewal, which relies on stem and progenitor cells.[1] To coordinate epithelium homeostasis, the corneal microenvironment is composed of epithelial cell-cell communication, dense innervation, and tear film. The latter is the source of corneal hydration and of nutrients for the epithelium.[2] Moreover, following the occurrence of a wound, the tear composition changes to support corneal wound healing through a modification of the factors secreted by the lacrimal gland (LG).[3] An altered tear film, which exhibits an imbalanced composition and offers fewer nutrients and growth factors to the corneal epithelium, affects corneal homeostasis. Persistent epithelial defects consequently appear, leading to impaired sight.[4] The change in tear composition requires an efficient sensory network in the cornea. The dense corneal innervation is essential for the maintenance of the corneal physiology. The neurotrophic factors, such as nerve growth factor (NGF), vasoactive intestinal peptide (VIP) or substance P (SP), released by the nerves for the epithelium, are crucial for homeostasis and wound healing.[5] A partial or complete loss of corneal innervation leads to a condition called neurotrophic keratitis (NK), which is characterized by a defective corneal homeostasis and arises from a lack of neurotrophic factors. This condition ultimately leads to corneal ulceration and perforation.[6] NK can result from full corneal transplant (severing all nerves), neurodegenerative diseases, or chronic metabolic diseases, such as diabetes. Currently, 415 million adults worldwide are diagnosed with diabetes, and the World Health Organization has projected that there will be 640 million such adults by 2040.[7] While underdiagnosed, diabetic keratopathy affects 47%–64% of diabetic adults.[8]

Current treatments for these corneal defects are topical, and consist of the application of eyedrops, which can be supplemented with autologous serum[9] or NGF.[10] Not only do these treatments prove onerous for patients, especially as regards the autologous serum, but the frequent lack of patient compliance with a prescribed eyedrop regimen actually leads to increased sight defects.[11]

These treatments rely solely on the application of an external eyedrop solution that mimics the tear film composition without considering the contribution of the LG, which produces, secretes, and modulates the tear film composition. Consequently, using LG directly as a

Received 7 June 2022; accepted 18 August 2022;
https://doi.org/10.1016/j.omtm.2022.08.006.

Correspondence: Benoit Gautier, Institute for Neurosciences of Montpellier, University of Montpellier, INSERM, Montpellier, France.
E-mail: benoit.gautier@inserm.fr
Correspondence: Frédéric Michon, Institute for Neurosciences of Montpellier, University of Montpellier, INSERM, Montpellier, France.
E-mail: frederic.michon@inserm.fr

bioreactor would constitute an appealing alternative strategy for the modulation of the tear film composition. This could be achieved by adenovirus-associated virus (AAV) vector-mediated gene transfer into LG. Indeed, AAV vectors present many advantages for gene delivery. They efficiently transduce a broad range of cells in which they allow long-lasting transgene expression. Significantly, they trigger limited/mild immunogenic responses *in vivo*, which indicates their overall biosafety.[12] Numerous AAV-based gene therapies have emerged, as evidenced by the large number of ongoing clinical trials, notably for neurodegenerative, neuromuscular, cardiovascular, and ocular genetic diseases, and for cancer.[13,14] To date, only two AAV-based gene therapies have been approved by the US Food and Drug Administration (FDA). Luxturna (voretigene neparvovec) is used for the treatment of biallelic RPE65 mutation-associated retinal dystrophy,[15] while Zolgensma (onasemnogene abeparvovec-xioi) is delivered to pediatric patients younger than 2 years who suffer from spinal muscular atrophy.[16] Significantly, in the field of ophthalmology, the majority of studies which use AAV-based gene delivery have to date focused on the retina and to a lesser extent on the cornea.[17,18] Very little data are currently available on AAV-based gene transfer into LG.[19,20] One report showed that AAV2/5 and AAV2/9 exhibit the greatest tropism for LG,[19] without demonstrating any effect on the tear film. A second report demonstrated that the use of an AAV2/2 to overexpress interleukin-10 (IL-10) could be used to treat LG inflammation,[20] but studied neither the chronology nor the dose effect of the AAV transduction.

In this study, we present a novel strategy for the modulation of corneal physiology by means of targeted tear film modification by transferring a gene of interest into LG. We confirmed that AAV-mediated gene transfer was feasible in murine LG using AAV2/5 or AAV2/9. Having demonstrated that all epithelial cell types are prone to AAV-mediated gene transfer, we used AAV2/5- and AAV2/9-mediated murine nerve growth factor (mNGF) as proof of concept to establish the parameters for efficient gene transfer, which would allow a targeted modification of tear composition. We chose mNGF because it is physiologically secreted in tears[21] and also because it is already used topically on the cornea of patients suffering from NK,[22] thus minimizing the risk of toxicity. We investigated the impact of AAV serotype on secreted protein levels and chose AAV2/9 vector to investigate the duration of tear film modulation, as well as possible negative consequences on the cornea itself of such an approach. Altogether, our results demonstrate that a single AAV2/9 injection into murine LG could be used to specifically modify the tear film, and consequently to reinforce corneal physiology in pathological contexts, such as NK.

RESULTS

AAV2/9 and AAV2/5 mediate an efficient gene transfer in the LG

To investigate the use of the LG as a bioreactor for protein secretion in the tear film, we established an injection protocol that allows an efficient AAV-mediated gene transfer after a single injection into murine LG. We used AAV2/9-CAG-GFP and AAV2/5-CAG-GFP to monitor the extent of vector diffusion within LG. The immunostaining of GFP demonstrated that these AAV serotypes induced GFP expression in all territories of the LG (Figure 1), but not all of the LG cells were positive (Figure 2, blue arrowheads). To rule out a possible tropism of AAV serotypes for a specific cell type, we looked at GFP expression, 1 month after injection, in two different LG epithelial cell populations, namely the E-cadherin-positive (E-cadh$^+$) cells, located in the acinar compartment, and the keratin19$^+$ (Krt19$^+$) subpopulation, specifically localized in the ducts.[23] The GFP/E-cadh co-labeling showed that almost all acinar cells were GFP$^+$ regardless of the used serotype (Figures 2A and S1). Similarly, the GFP/Krt19 co-labeling demonstrated that most of the ductal cells were GFP$^+$ after AAV2/9-CAG-GFP and AAV2/5-CAG-GFP injection (Figures 2B and S2).

To evaluate a possible discrepancy between AAV serotypes 2/5 and 2/9 in the transduction efficiency, we analyzed by western blot the levels of GFP protein expressed in LG after injection of AAV2/9- or AAV2/5-CAG-GFP (Figure 3). As expected, while in the LG injected with AAV2/9 or AAV2/5 empty capsids, no GFP protein was detected (Figure 3A), high levels of GFP were detected in the LG injected with AAV2/9 or AAV2/5-CAG-GFP, respectively. Interestingly, when comparing the two AAV serotypes, GFP levels were found to be significantly higher after AAV2/9-CAG-GFP injection than after AAV2/5-CAG-GFP injection (Figure 3B).

Taken together, our results demonstrate that the LG can be widely transduced by AAV2/9 and AAV2/5, and that serotype 2/9 exhibits a higher transduction efficiency.

The transgene expression leads to the secretion of the resulting protein in the tear film

To evaluate whether AAV2/9 and AAV2/5 serotypes have a different impact on the amount of protein secreted in the tear film, we chose to express the mNGF in the LG, using either AAV2/9 (AAV2/9-CAG-mNGF) or AAV2/5 (AAV2/5-CAG-mNGF). Following AAV injection into the LG, the transgene expression should lead to the secretion of mNGF in the tear film. To assess this secretion, we measured mNGF level in the tear film using ELISA (Figure 4) and western blot analyses (Figure 5A). Tear film contains a basal level of mNGF,[21] which can have two forms.[24,25] The pro-mNGF, of higher molecular weight, is cleaved to generate the mature mNGF, the active form. As expected from the GFP results, injection of AAV2/9 and AAV2/5 CAG-mNGF induced a significant increase in the mNGF levels in the tear film, whereas only endogenous basal expression levels of mNGF were detected with the empty AAV vectors. Moreover, consistent with the GFP expression data in the LG, the mNGF amount in the tear film was more than 3-fold higher after AAV2/9 injection than after AAV2/5 injection (Figure 4). Moreover, western blot analysis confirmed that the injection of AAV2/9 and AAV2/5 CAG-mNGF led to a significant increase in the total mNGF level in the tear film (Figures 5A and 5B). Importantly, this analysis revealed that mNGF was consistently found in the tear film in its pro-mNGF form (Figure 5C). However, the analysis of the mature mNGF showed a maturation process (Figure 5D). Indeed, the mature mNGF form was close to absent from the tear film of mice injected in LG with empty AAV2/9 or AAV2/5, whereas a large amount of mature

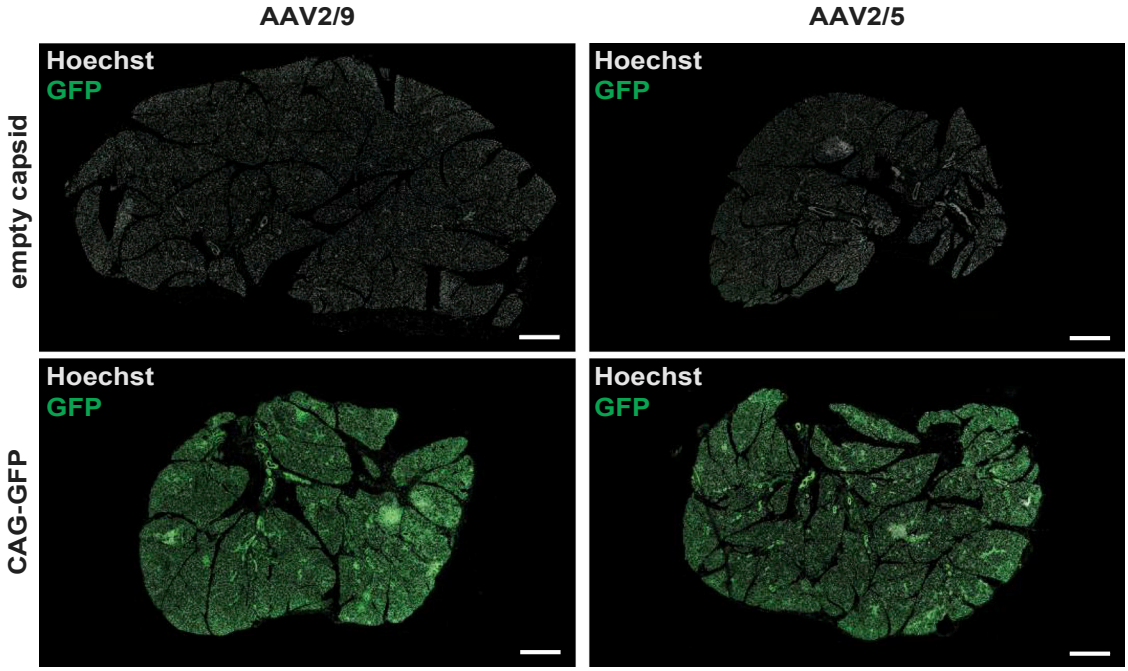

Figure 1. AAV2/9 and AAV2/5-CAG-GFP transduce widely the murine LG

Representative images of LG longitudinal sections show GFP protein (green) following a single injection of AAV2/9 or AAV2/5-CAG-GFP into murine LG, when compared to AAV2/9 or AAV2/5 empty capsid-injected mice, respectively (10^{10} vg/LG in 3 μL, n = 3 mice per group). Mice were sacrificed 1 month post-injection. Nuclei are counterstained with Hoechst 33342 (white). Scale bar: 500 μm.

mNGF was detected after AAV-mNGF gene transfer. Notably, AAV2/9-CAG-mNGF gave rise to four times more of the mature form than with AAV2/5-CAG-mNGF injection (Figure 5D).

AAV2/9-mediated gene transfer induces a dose-dependent and long-term protein secretion

Consequent to our results indicating a better protein secretion using AAV2/9 compared to AAV2/5, we chose to focus on the serotype 2/9. To establish the optimal amount of vector genomes (VGs) to be injected in the LG, we tested three doses and checked the amount of secreted mNGF 1 month after injection (Figure 6A). While injection of 10^9 VGs did not lead to a drastic increase in the mNGF secretion, a single injection of 10^{11} VGs induced the secretion of 75 ng mNGF per milliliter of tear film. We compared this concentration to the physiological increased mNGF secretion observed after corneal injury.[26] After AAV2/9 injection, we obtained a concentration representing a 10× increase in comparison to physiological mNGF secretion during the cornea wound healing process, in which a concentration of 7.5 ng/mL was found 7 days after abrasion (Figure S3). We concluded that 10^{11} VG/LG was suitable to have a significantly high increase in the protein secretion in the tear film.

Subsequently, we evaluated the dynamics of the mNGF secretion over a 6-month period (Figure 6B). The injection of 10^{11} VGs into the LG induced a significant increase in the mNGF level found in the tear film already after 1 week, before reaching a peak at 30 days post-injection. The mNGF secretion then decreased to reach a plateau 120 days after injection, with stable expression during the 60 following days. However, although injection of 10^{10} VG/LG of AAV2/9-CAG-mNGF or AAV2/5-CAG-mNG induced a peak 30 days after injection, only the serotype 2/9 induced a significant increase in the mNGF level in the tear film (Figure S4). Nonetheless, the secreted mNGF level for both serotypes decreased and were no more different than the basal level. Taken together, these results show the long-lasting protein secretion when injecting 10^{11} VG/LG, compared to 10^9 or 10^{10} VGs, and confirm that AAV2/9 is more efficient than AAV2/5.

AAV2/9 VG copies in the murine LG correlates with the amount of protein secreted in the tear film

To further analyze the use of 10^{11} VG/LG, we investigated the biodistribution of the AAV2/9-CAG-mNGF vector after injection into LG. We measured the amount of VGs per diploid genome (DG) in LG, liver, and heart 1 month after vector injection (Figure 7A). All of the injected mice showed VG copies in the LG, indicating that the injection technique is reliable and reproducible. Interestingly, we found approximately 0.25 VG/DG in the LG, meaning that an average of 1 of 4 cells was transduced with 1 copy of the AAV2/9-CAG-mNGF vector, which reflects an efficient gene transfer. Despite the detection of the AAV2/9-CAG-mNGF VG in the liver and heart of injected mice, the levels were very low to negligible, with 14 and 80× fewer vector genomes/diploid genome in the liver and heart, respectively, than in the LG.

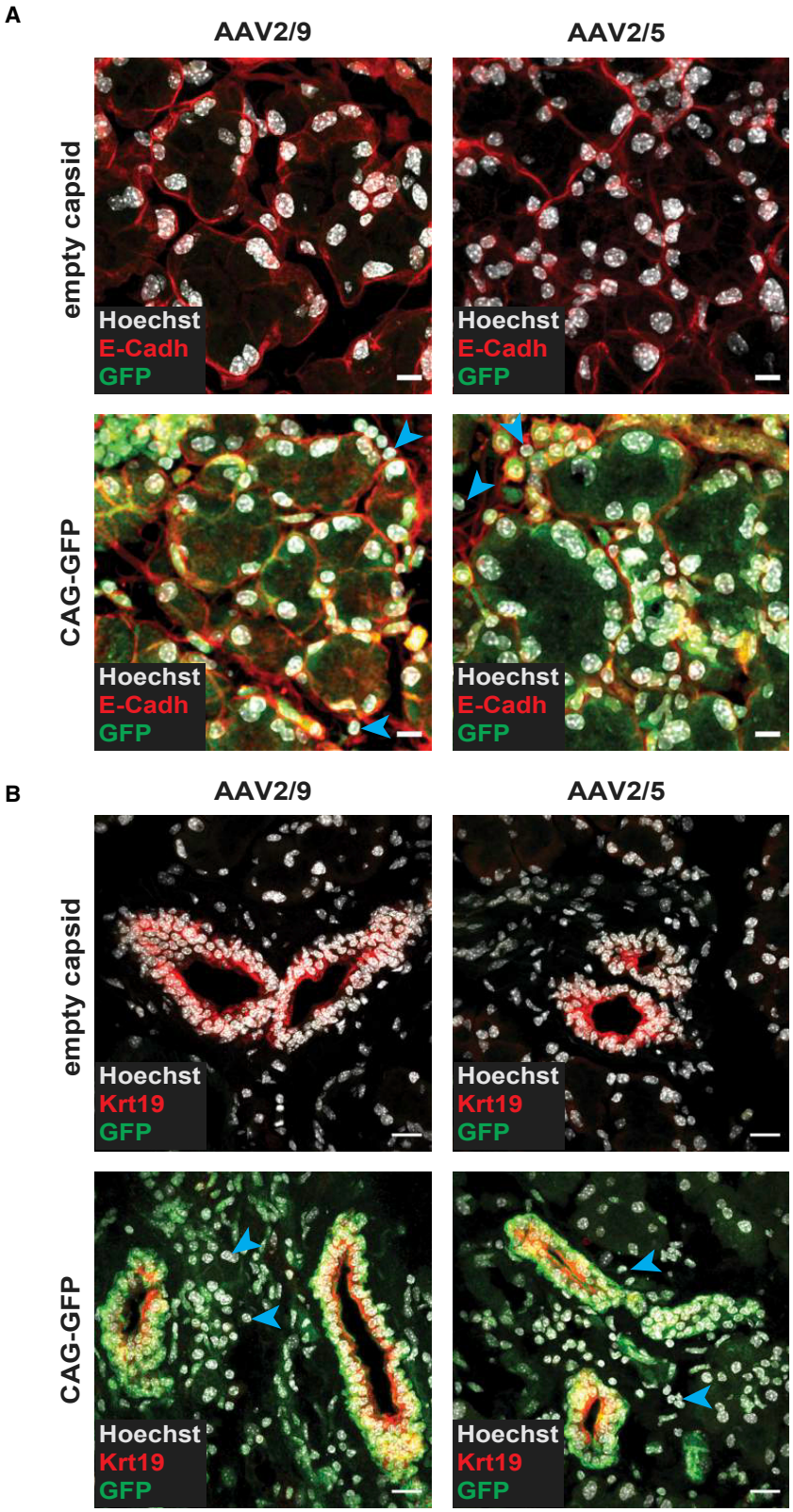

Figure 2. AAV2/9 and AAV2/5-CAG-GFP transduce LG acinar and ductal cells

Representative images of LG longitudinal sections show GFP protein (green) in acinar cells immunostained for E-cadh (red, A) and in ductal cells immunostained for Krt19 (red, B) after a single injection of AAV2/9 or AAV2/5-CAG-GFP into murine LG, when compared to AAV2/9 or AAV2/5 empty capsid-injected mice, respectively (10^{10} VG/LG in 3 μL, n = 3 mice per group). Mice were sacrificed 1 month post-injection. Nuclei are counterstained with Hoechst 33342 (white). Blue arrowheads highlight some GFP^{-} cells. Scale bar: 10 μm (A) and 20 μm (B).

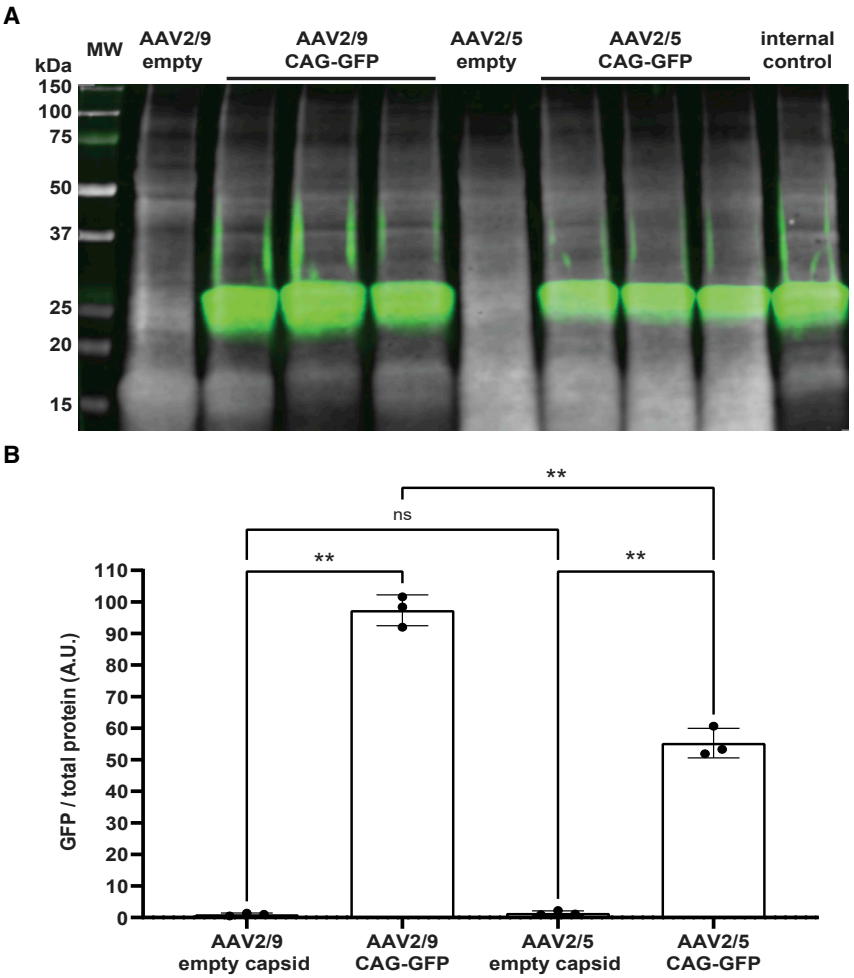

Figure 3. GFP is detected in AAV2/9 and AAV2/5-CAG-GFP-injected LG and dosed by western blot

GFP protein levels were analyzed by western blot experiments in the murine LG lysates of AAV2/9 or AAV2/5-CAG-GFP-injected mice, when compared to AAV2/9 or AAV2/5 empty capsid-injected mice, 1 month post-injection, respectively (10^{10} VG/LG in 3 μL, n = 3 mice per group), 1 month post-injection (A). Representative western blot image showing GFP level (green) and total protein as loading control (white) in murine LG lysates of injected mice. (B) Quantification of GFP/total protein ratio in LG lysates. Results are expressed as the mean ± SD. Statistical analysis using Brown-Forsythe and Welch ANOVA tests followed by Dunnett's T3 multiple comparisons test. **p = 0.0026 between AAV2/9 empty capsid and AAV2/9 CAG-GFP groups, **p = 0.0077 between AAV2/5 empty capsid and AAV2/5-CAG-GFP groups, and **p = 0.0018 between AAV2/9-CAG-GFP and AAV2/5-CAG-GFP groups. ns, not significant; A.U., arbitrary units.

Then, we compared the vector genome/diploid genome values to the concentration of mNGF in the tear film of the same injected mice (Figure 7B). Remarkably, we found a nice correlation between the vector genome/diploid genome values detected in the LG and the amounts of secreted mNGF in the tears. The increase in vector genome/diploid genome value corresponded to a higher mNGF secretion.

Taken together, these results confirm the high transduction efficiency displayed by AAV2/9, which is additionally correlated with the amount of protein secreted in the tear film. Moreover, they showed a very limited distribution of AAV2/9 vector to peripheral organs after a single injection into murine LG.

AAV2/9-mediated mNGF secretion does not affect corneal integrity

After resolving the parameters for an efficient AAV2/9-mediated mNGF gene transfer, its biodistribution, and induced mNGF secretion, we investigated the impact of the mNGF over secretion on LG physiology and corneal integrity. We injected 10^{11} VG/LG of AAV2/9-CAG-mNGF and measured the impact on tear volume and protein concentration in tears over a period of 8 months. (Figures 8A and 8B). Simultaneous with the increase in mNGF secretion (Figures 4, 5, and 6), we detected a significant increase in the tear volume from 7 to 60 days post-injection when compared to the injection of AAV2/9 empty capsid (Figure 8A). Interestingly, this increase in the tear volume was matched with a stability of the protein concentration in tears (Figure 8B). Moreover, to rule out any negative impact of the injection procedure on LG physiology, we analyzed the tears before and after the AAV2/9 empty capsid injection (Figures S5 and S6). Importantly, after injection of the AAV2/9 empty capsid and during the whole 8-month period, no modification of tear volume or of total protein concentration was observed (Figures S5 and S6), except at the 6th and the 8th month, in which the tear flow was increased, reflecting a possible impact of aging.[27] This observation rules out any deleterious impact of the injection procedure itself on LG physiology.

In addition, we used fluorescein staining to monitor the corneal epithelium integrity and visualize any adverse effect that the injection procedure and the tear film modification could have on the cornea. Fluorescein stains areas where the corneal epithelial barrier is defective,[1] such as after corneal abrasion (Figure 8C). During the 240 days after AAV2/9 injection, we never observed any fluorescein staining, whether we injected an empty capsid or induced mNGF over secretion. We concluded that AAV2/9 injection does not affect the corneal epithelium integrity.

To investigate further the effect of the mNGF over secretion on the cornea, we visualized corneal innervation with βIII-tubulin

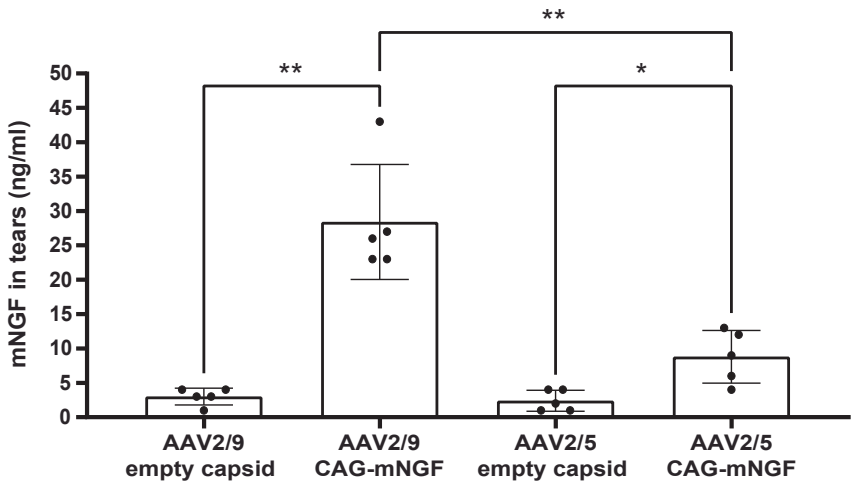

Figure 4. Injections of AAV2/9 and AAV2/5-CAG-mNGF into murine LG significantly increase the level of mNGF in tears

mNGF protein levels (ng/mL) were measured by ELISA in the tears of AAV2/9 or AAV2/5-CAG-mNGF-injected mice, when compared to AAV2/9 or AAV2/5 empty capsid-injected mice, 1 month post-injection, respectively (10^{10} VG/LG in 3 μL, n = 5 mice per group). Results are expressed as the mean ± SD. Statistical analysis using Brown-Forsythe and Welch ANOVA tests followed by Dunnett's T3 multiple comparisons test. **p = 0.0065 between AAV2/9 empty capsid and AAV2/9-CAG-mNGF groups, *p = 0.0464 between AAV2/5 empty capsid and AAV2/5-CAG-mNGF groups, and **p = 0.0085 between AAV2/9-CAG-mNGF and AAV2/5-CAG-mNGF groups.

immunolabeling, which is a pan-neuronal marker. We showed that the gross morphology of corneal fibers was not affected by the oversecretion of mNGF in the tear film (Figure 9A). Furthermore, we performed von Frey tests on the corneas of injected mice. We demonstrated that the constant oversecretion of mNGF did not modify corneal sensitivity (Figure 9B). Altogether, these results demonstrate that the injection procedure and mNGF oversecretion respect the LG physiology and the corneal integrity.

DISCUSSION

Corneal defects are the fourth most prevalent cause of blindness worldwide. Among the most prominent causes of corneal defects, three are among the leading causes for hospital patient influx. The first of these is physical injury to the eye, such as abrasions,[28] which are caused by small foreign objects that scratch the epithelium.[29] Dry eye diseases (DEDs) account for the second leading cause of corneal defects, in which the loss of physiological tear film is the central pathophysiological element.[30] DEDs can arise from genetic diseases, such as Gougerot-Sjögren's syndrome,[31] or from aging, with up to one-third of the elderly population being affected.[27,32] The third leading cause of corneal defects is NK, which is often associated with corneal microenvironment dysregulation.[33]

The aim of this study was to establish an innovative and attractive strategy to tackle corneal defects by sustainably modulating the tear film composition. Tear film originates mainly from the LG for the aqueous part, and from the Meibomian glands for the lipidic part, which is on the external side of the eye. While acknowledging that modulating the lipidic part may be beneficial for evaporative DED, we chose to modulate the aqueous part of the tear film. For this purpose, we chose an AAV-mediated gene transfer to use LG as a bioreactor producing specific transgenes. Nevertheless, several major variables are crucial in the realization of an efficient transduction of the target cells, and this process must therefore be particularly well designed.[12,34] The route of administration determines both the efficacy and the biosafety pattern of an AAV-based gene transfer. In this study, we used a local injection into the LG, as this organ is easily accessible by surgery. Moreover, we showed that a local injection augments the concentration and persistence of AAV vectors specifically within the vicinity of the target cells and limits the biodistribution of the vector to non-targeted tissues, thus limiting the risk of toxicity. Local injection is already a well-established strategy for ocular diseases, particularly in retinal disorders, with several anatomical sites being typically targeted: subretinal, intravitreal, intracameral, suprachoroidal, and topical.[35,36] Furthermore, the injection method is a key parameter in attaining a high level of diffusion within the target organ. While a systemic injection leads to a large diffusion throughout the organism, including the target organ,[37] specific injection procedures must be developed when local injection is used. For example, the use of several injections at precise coordinates is required to achieve a large diffusion within the brain.[38] Interestingly, a pneumatic picopump system applying multiple short-time pressure pulses has been reported as transducing the entire sciatic nerve of rodents.[39] In this study, we used a 34G beveled needle linked to a 10-μL Hamilton syringe to perform injections into the LG. We injected 3 μL of AAV vectors by following the path of the LG main duct. This injection procedure led to a large diffusion within the gland, and showed an efficient gene transfer in all of the epithelial cell types in the murine LG. This procedure will require specific adjustments if used in larger animals.

The promoter used to drive the expression of the transgene is a second parameter that determines the transduction efficiency and biosafety pattern of the injection.[12,34] Indeed, the promoter controls the transgene expression level. AAV-mediated gene transfer typically uses an ubiquitous and strong promoter, such as cytomegalovirus (CMV) enhancer fused to the chicken β-actin promoter (CAG) and CMV, to achieve high transgene expression.[40,41] Moreover, researchers usually use such promoters when trying to establish a proof of concept for AAV-mediated gene transfer into a specific organ. In this study, we used a CAG promoter to provide a proof of concept of the tear fluid composition modulation after an AAV-mediated gene transfer into murine LG. However, a high transgene expression level is not always desired. For instance, the toxicity of transgene overexpression over physiological levels has been reported.[42] This toxicity must be

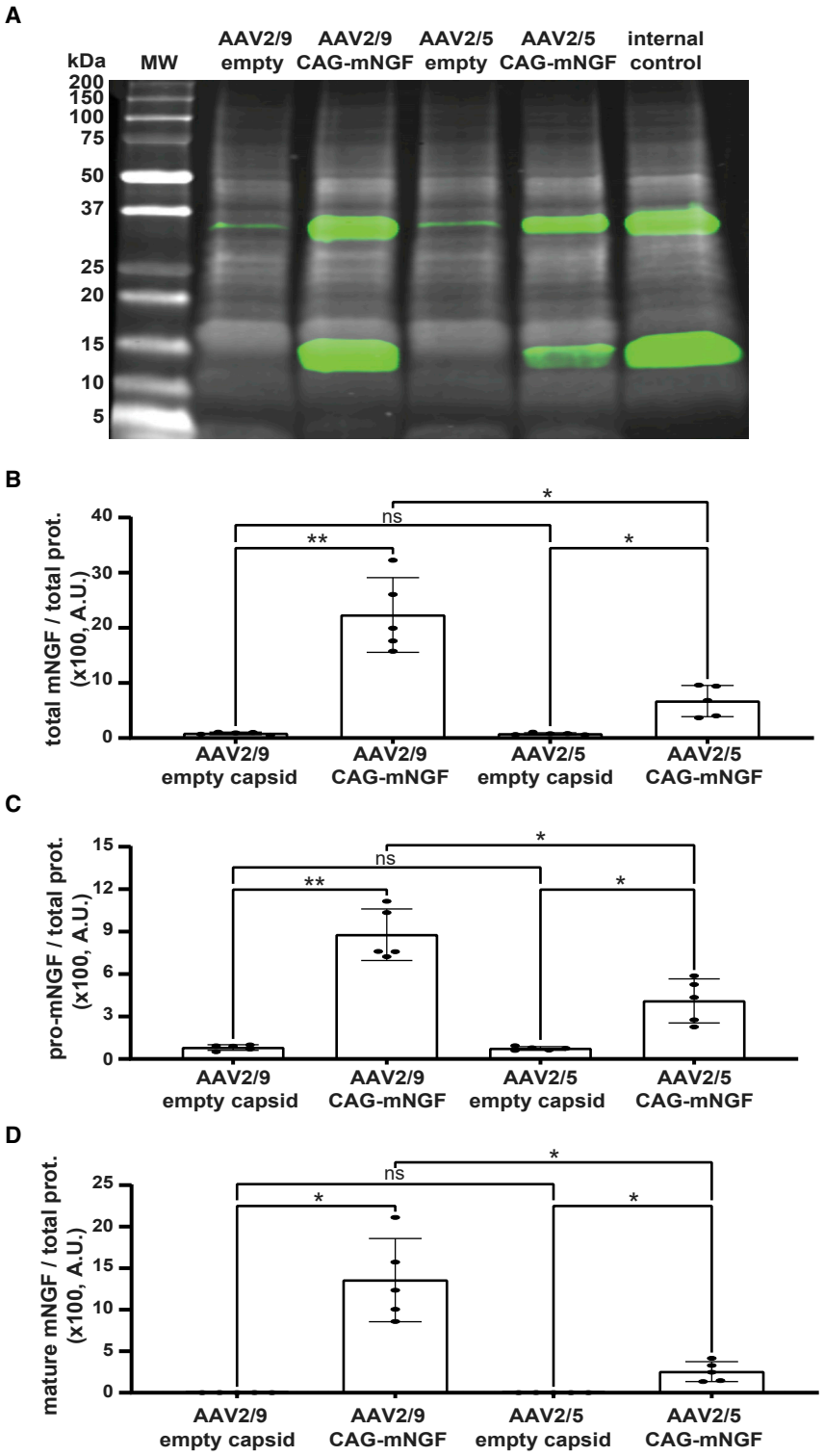

Figure 5. Injections of AAV2/9 and AAV2/5-CAG-mNGF into murine LG significantly increase the level of total, pro-, and mature mNGF in tears

mNGF protein levels were analyzed by western blot experiments in the tears of AAV2/9 or AAV2/5-CAG-mNGF-injected mice, when compared to AAV2/9 or AAV2/5 empty capsid-injected mice, 1 month post-injection, respectively (10^{10} VG/LG in 3 μL, n = 5 mice per group). (A) Representative western blot image showing mNGF level (green) and total protein as loading control (white) in the tears of injected mice. Relative quantification of total mNGF (B), pro-mNGF (C), and mature mNGF (D) protein levels in the tears of injected mice Results are expressed as the mean ± SD. Statistical analysis using Brown-Forsythe and Welch ANOVA tests followed by Dunnett's T3 multiple comparisons test. (B) **p = 0.0091 between AAV2/9 empty capsid and AAV2/9-CAG-mNGF groups, *p = 0.0397 between AAV2/5 empty capsid and AAV2/5-CAG-mNGF groups, and *p = 0.0235 between AAV2/9-CAG-mNGF and AAV2/5-CAG-mNGF groups. (C) **p = 0.0027 between AAV2/9 empty capsid and AAV2/9-CAG-mNGF groups, *p = 0.0363 between AAV2/5 empty capsid and AAV2/5-CAG-mNGF groups, and *p = 0.0127 between AAV2/9-CAG-mNGF and AAV2/5-CAG-mNGF groups. (D) *p = 0.0162 between AAV2/9 empty capsid and AAV2/9-CAG-mNGF groups, *p = 0.0388 between AAV2/5 empty capsid and AAV2/5-CAG-mNGF groups, and *p = 0.0368 between AAV2/9-CAG-mNGF and AAV2/5-CAG-mNGF groups.

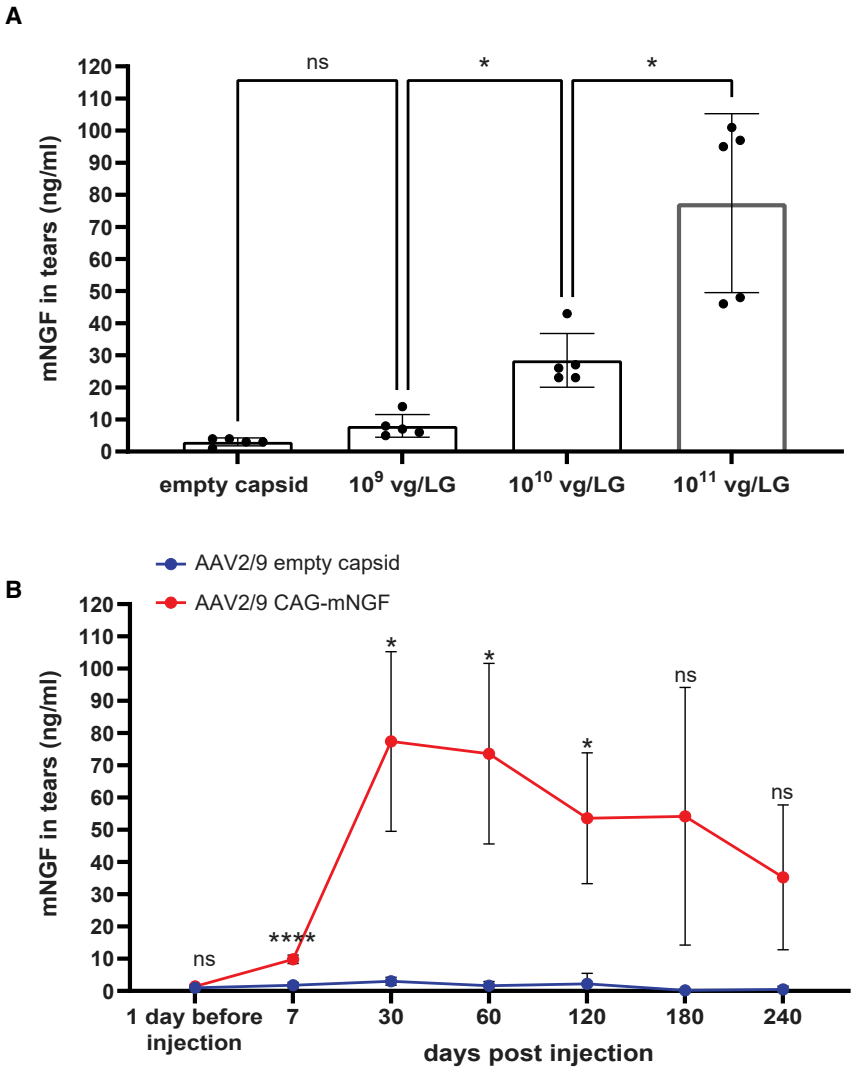

Figure 6. Dose-response and kinetic studies after injection of AAV2/9-CAG-mNGF into murine LG reveal a high and long-lasting secretion of mNGF in tears

For the dose-response study, mNGF levels were analyzed by ELISA in the tears of AAV2/9-CAG-mNGF-injected mice by increasing dose of vectors (10^9, 10^{10}, and 10^{11} VG/LG in 3 μL, n = 5 mice per dose), when compared to the tears of AAV2/9 empty capsid-injected mice 1 month post-injection. For the kinetic study, mNGF levels were analyzed by ELISA in the tears of AAV2/9-CAG-mNGF-injected mice (10^{11} VG/LG in 3 μL), when compared to the tears of AAV2/9 empty capsid-injected mice, 1 day before injection and at 7, 30, 60, 120, 180, and 240 days post-injection (n = 5 mice per group, except at 240 days post-injection n = 4). (A) Quantification by ELISA of mNGF level (ng/mL) in the tears of injected mice at the indicated doses. Results are expressed as the mean ± SD. Statistical analysis using Brown-Forsythe and Welch ANOVA tests followed by Dunnett's T3 multiple comparisons test. *p = 0.0107 and *p = 0.0341 between the doses 10^9 and 10^{10} VG/LG and between the doses 10^{10} and 10^{11} VG/LG, respectively. (B) Quantification by ELISA of mNGF level in tears (ng/mL) at the indicated days post-injection. Results are expressed as the mean ± SD. Statistical analysis using mixed-effects analysis followed by Sidak's multiple comparisons test. ****p < 0.0001, *p =0.0270, *p =0.0311, and *p =0.0297, between AAV2/9 empty capsid and AAV2/9-CAG-mNGF groups at 7, 30, 60, and 120 days post-injection, respectively.

correlated to the serotype of the AAV vector. Indeed, the serotype represents yet another parameter that influences both the transduction efficiency and the biosafety of an injection, as each AAV serotype exhibits different cell and tissue tropisms.[43] Therefore, the combination of the route of administration, the AAV serotype, the promoter driving the transgene expression, and the vector dose must be carefully designed, as this combination may induce transgene expression in off-target tissues and thus lead to dramatic toxicities.[44] In this study, we compared the use of AAV serotypes 2/5 and 2/9 first to transduce the murine LG and then to modulate the tear film composition. It was notable that while both serotypes led to an efficient gene transfer in the LG, AAV2/9 gave a better yield of GFP production and mNGF secretion, as compared with AAV2/5. In the LG, the high GFP production should be considered in the context of a secretory organ. Indeed, the GFP was earlier shown to label cells that did not have the GFP DNA, whether through mRNA moving from one cell to another via membrane structural extensions[45] or GFP-loaded exosomes being internalized in distant cells. This form of cell-cell communication is relatively common.[46,47]

While the difference in transduction efficiency had been reported previously,[19] the 2- to 4- fold increase in mNGF secretion was nonetheless startling. Indeed, until now, no study has reported a transgene secretion in the tear fluid after an AAV-mediated gene transfer into murine LG. Furthermore, we tested increasing the dose of AAV2/9 to evaluate the mNGF secretion in the tear film. Interestingly, while a 10^{11} VG/LG dose led to the highest and longest mNGF secretion, 10^{10} VG/LG was sufficient to induce a significant secretion. This observation could reflect the need for fine-tuning the dosage according to the pathology being treated.

Given that we used the serotype 2/9, which is known to show high heart and liver tropism in rodents[48] and known as a strong CAG promoter, we performed a biodistribution study for AAV2/9. This study was paramount in determining the potential off-targets of our strategy, which may lead to both unwanted toxicity and immunogenicity. At the highest injected dose of 10^{11} VG/LG, we showed an average of 0.25 VG/DG in LG, only 0.017 VG/DG in the liver, and 0.003 VG/DG in the hearts of injected mice, corresponding to 14 and 80× less vector genomes/diploid genome than in LG, respectively. Significantly, these levels of AAV2/9 found in the liver and heart were very low to

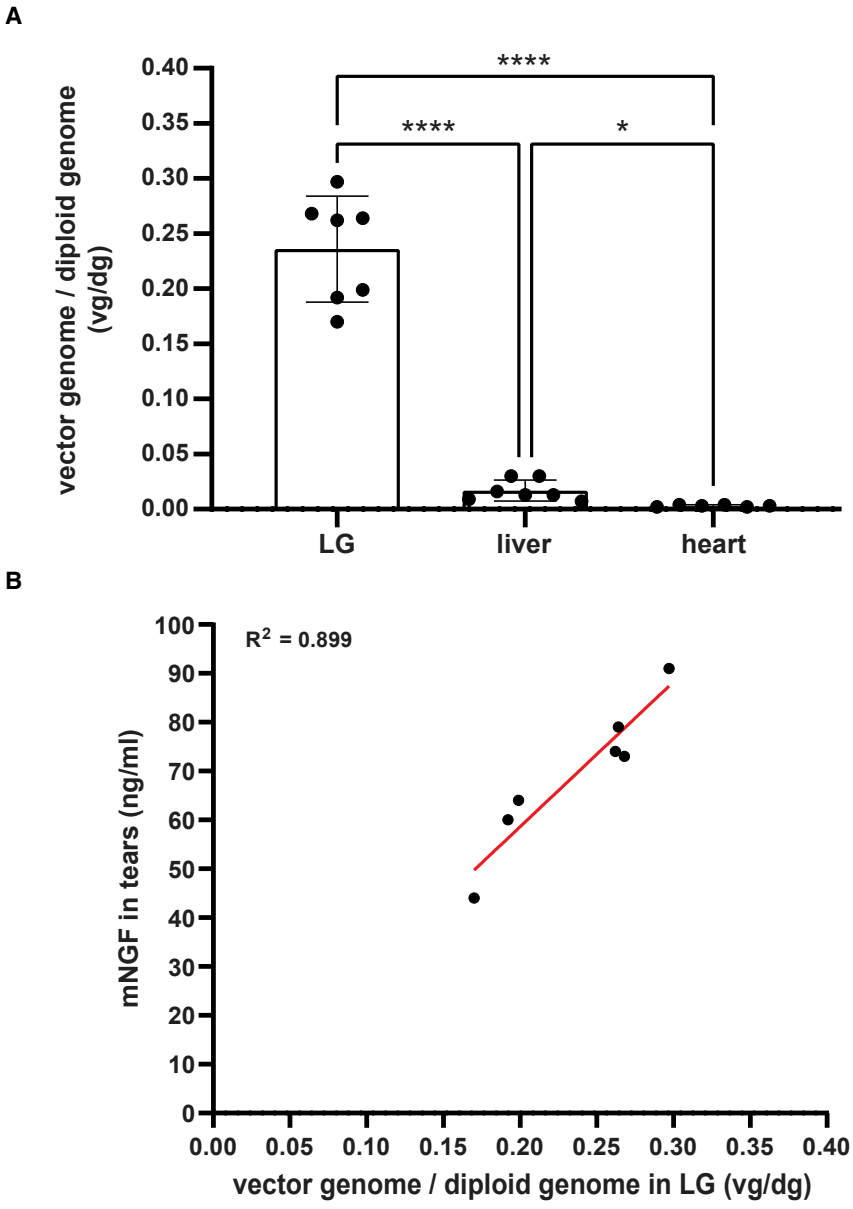

Figure 7. Biodistribution analysis after injection of AAV2/9-CAG-mNGF into murine LG reveals a limited diffusion to peripheral organs

AAV2/9-CAG-mNGF was injected into the murine LG (10^{11} VG/LG in 3 μL, n = 7 mice). One month post-injection tears were collected, and the mNGF level was quantified by ELISA. At the same time mice were sacrificed, LG, liver, and heart were collected and analyzed by qPCR. (A) Quantification of the transduction rate expressed in VG/DG above the lowest limit of quantification (LLOQ) (n = 7 for LG and liver samples, n = 6 for heart samples). Results are expressed as the mean ± SD. Statistical analysis using Brown-Forsythe and Welch ANOVA tests followed by Dunnett's T3 multiple comparisons test. ****$p < 0.0001$ between LG and liver, ****$p < 0.0001$ between LG and heart, and *$p = 0.0226$ between liver and heart. (B) Graph showing the statistical linear regression (red line) for each mouse between mNGF level (ng/mL) in tears and VG/DG in LG.

negligible, being 100–10,000× lower than those obtained after intravenous[41] or intrathecal[49] injections.

Different strategies exist to limit the transgene expression in off-targets and related adverse effects. Such strategies include the use of cell-type-specific promoters[41] and the incorporation of microRNA (miRNA) binding sites in the AAV gene expression cassette.[50] We can speculate that the use of a 10× lower dose of AAV2/9 vector, providing a high secretion of mNGF, could bring about a lower off-target transduction. Injection of 10^{10} VG/LG of AAV led to a faster secretion of mNGF with AAV2/9 compared to AAV2/5. After a peak 30 days post-injection, the mNGF secretion decreased to the physiological level with both serotypes. Injection of 10^{11} VG/LG, however, results in the oversecretion of mNGF for a period of several months. This is an important consideration for the subsequent use of this method, insofar as it suggests that a lower dose could be used for transitory pathologies such as corneal graft or recurrent corneal abscesses, while a higher dose could be beneficial for chronic pathologies, such as NK, or DEDes. However, this approach would not be suitable in the context of a defective LG, such as seen in Gougerot-Sjögren's syndrome, in which the LG failure is due to an autoimmune condition.[51]

The long-term secretion of mNGF is a remarkable discovery and must be linked to LG physiology. Like all epithelial organs, such as skin, cornea, or mammary glands, the epithelial compartment contains stem cells that continuously regenerate the organ, as well as heal it, if necessary.[52] The AAV vector is a non-integrative vector that can be lost when cell division occurs.[53] Even if a large majority of AAV VGs can persist within the transduced cells as episomes, it cannot be excluded that a fraction of them may integrate the host genome. There are consequently two possible explanations for the longevity of the mNGF secretion that we observed with AAV2/9: (1) AAV2/9 transduced numerous long-lived non-proliferative cells. (2) AAV2/9 transduced LG epithelial stem cells in which the VG is integrated, providing the construct to their daughter cells. Both possibilities are of course valid, and we cannot currently favor one over the other. Moreover, no study to date has demonstrated the turnover of the adult LG epithelium. Our results demonstrate that gene therapy is successful on this epithelial organ and highlights the low turnover of epithelial cells in the LG. Knowing that there was approximately 1 AAV2/9 vector genome in every 4 cells 30 days after injection, it would be of great interest to monitor these levels over a

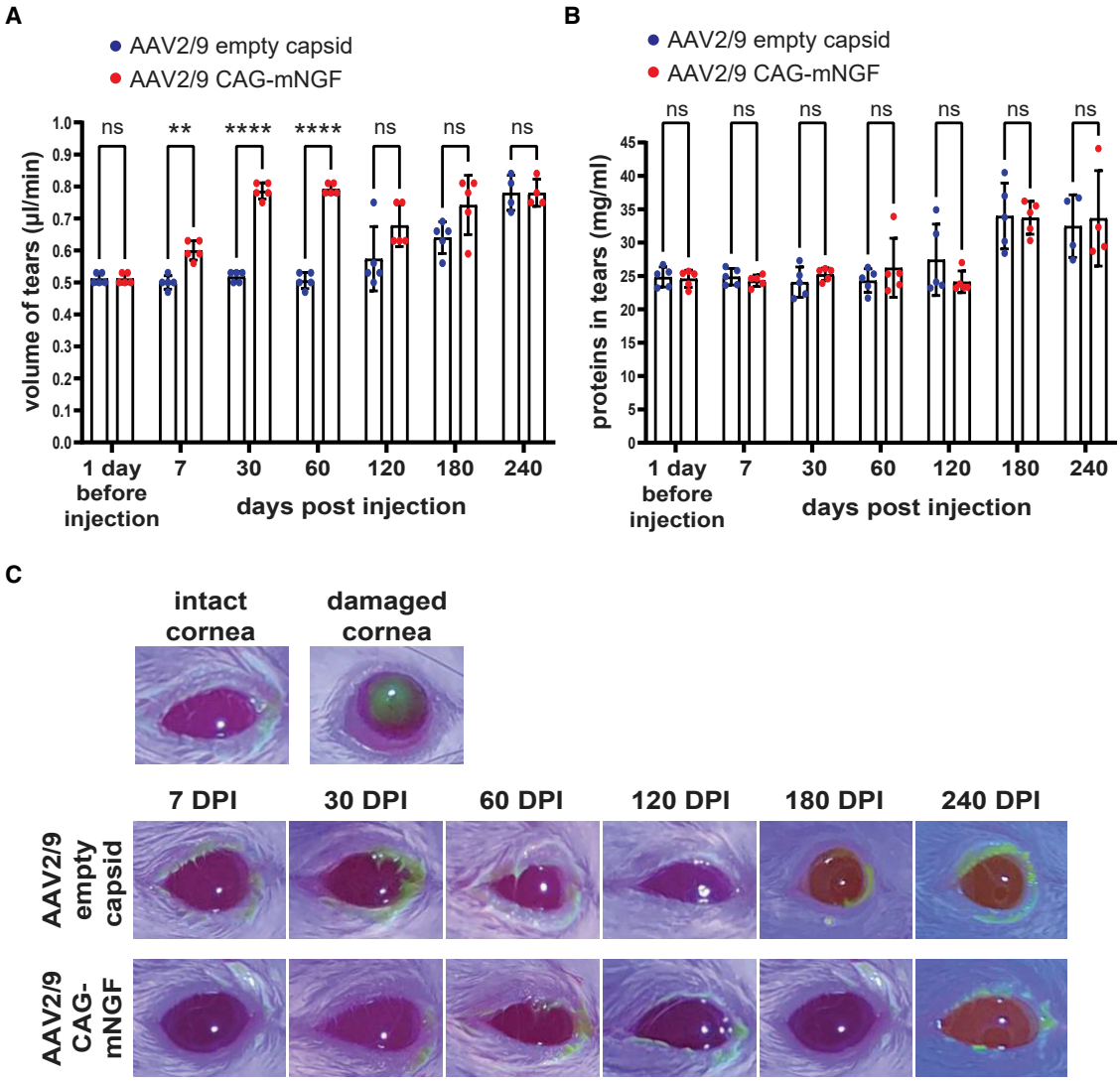

Figure 8. Injection of AAV2/9-CAG-mNGF into murine LG does not alter tear protein concentration or corneal integrity

AAV2/9 empty capsid or AAV2/9-CAG-mNGF were injected into murine LG (10^{11} VG/LG in 3 µL, n = 5 mice per group, except at 240 days post-injection n = 4). The volume of tears (A), the protein concentration in tears (B), and the corneal integrity (C) were assessed 1 day before injection and 7, 30, 60, 120, 180, and 240 days post-injection. (A) Graph showing the volume of tears (µL/min) collected before injection and at the indicated days post-injection. Results are expressed as the mean ± SD. Statistical analysis using mixed-effects analysis followed by Sidak's multiple comparisons test. **p = 0.0031 and ****p < 0.0001 between AAV2/9 empty capsid and AAV2/9 CAG-mNGF groups at 7, 30, and 60 days post-injection, respectively. (B) Graph showing the protein concentration in tears (mg/mL) collected before injection and at the indicated days post-injection. Results are expressed as the mean ± SD. Statistical analysis using mixed-effects analysis followed by Sidak's multiple comparisons test. (C) Eye images obtained from the fluorescein stain test. Fluorescein signal highlights an abraded cornea in bright green, while an intact cornea remains dark.

sustained period of time, to determine which cells retain the AAV2/9 genome. This would provide a deeper understanding of LG fundamental biology. Of course, such a long-term follow-up could only be made at the cellular level, as the LG physiology tends to be variously affected in different individuals due to the aging process.[27] Measuring tear volume and tear protein content could therefore be misleading, possibly being due more to the impact of aging than the AAV2/9 injection. Nevertheless, we demonstrated that up to 6 months after injection into the murine LG, our approach has no detrimental impact on LG physiology. However, we noted a significant increase in tear fluid secretion during the first 2 months after AAV2/9 injection. This observation can be correlated with a recent report showing that a treatment of recombinant human NGF eyedrops induces an increase in tear secretion,[54] confirming the functionality of our mNGF secretion in LG tear production.

The presence of mature mNGF in the tear film is important for its functionality. We showed that in the absence of mNGF oversecretion, only

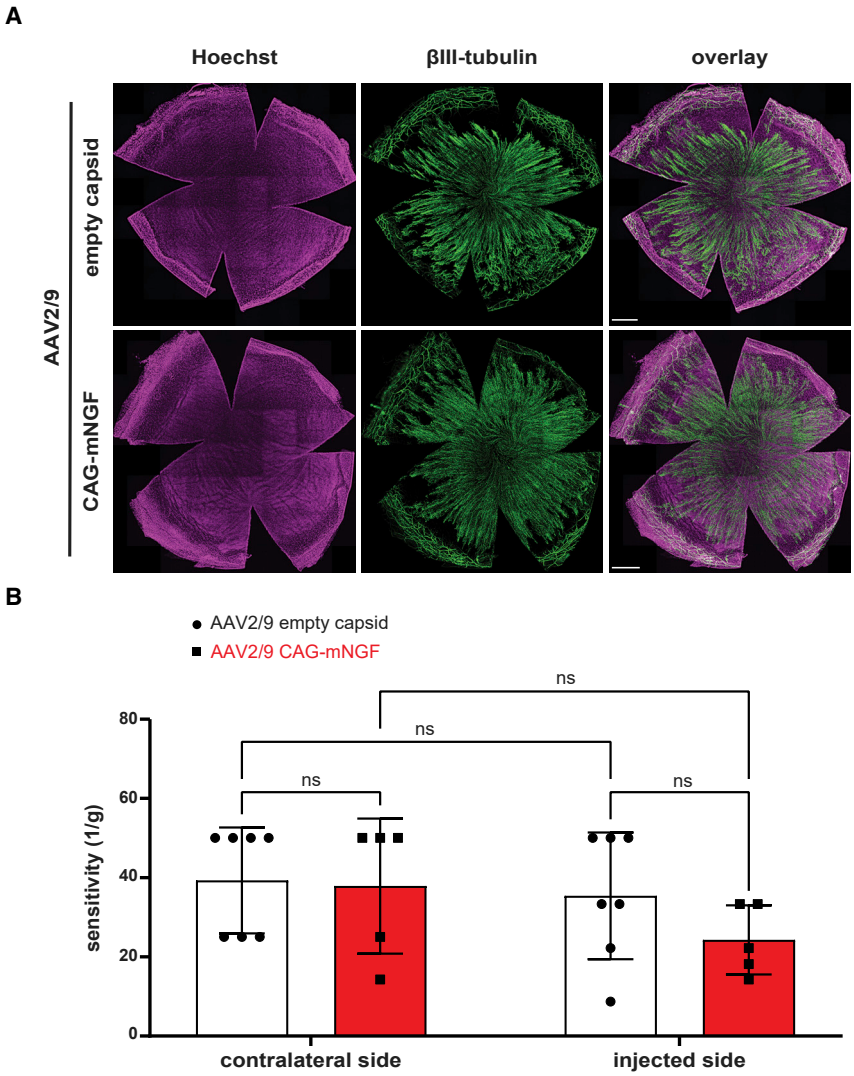

Figure 9. Injection of AAV2/9-CAG-mNGF into murine LG does not affect corneal innervation or sensitivity

(A) Representative images showing corneal innervation. Whole corneas were immunostained for βIII-tubulin (green) following a single injection of AAV2/9-CAG-mNGF into murine LG, when compared to AAV2/9 empty capsid-injected mice (10^{11} VG/LG in 3 μL, n = 3 mice per group). Mice were sacrificed 2 weeks post-injection. Nuclei are counterstained with BioTracker NIR694 (magenta). Scale bar: 500 μm. (B) Quantification of the corneal sensitivity (1/g) measured by von Frey test performed both on the contralateral side and the injected side of AAV2/9 empty capsid-injected (white plots, n = 7) or AAV2/9-CAG-mNGF-injected (red plots, n = 5) mice. von Frey analysis was performed 2 weeks post-injection. Results are expressed as the mean ± SD. Statistical analysis using 2-way ANOVA test followed by Sidak's multiple comparisons test.

a negligible part of the pro-mNGF was processed into its mature form. Interestingly, the mNGF oversecretion led to the presence of mature mNGF in the tears. However, we can offer no explanation as to why, after AAV2/9 injection, 57% of the total mNGF is matured, while only 34% is matured after AAV2/5 injection. We can only hypothesize a threshold effect leading to better pro-mNGF processing into mature mNGF when there is an increase in secretion in the tear film.

Despite the large amount of mNGF and its constant presence on the cornea, we did not detect any impact on corneal innervation or on corneal sensitivity. We hypothesize that the robustness of corneal innervation keeps the system under control in physiological conditions, and that mNGF alone is not sufficient to disturb this. Under pathological conditions (i.e., physical harm or neurotrophic keratopathy), it is likely that the system would be sufficiently perturbed that the effect of mNGF on corneal innervation could be detected.

Current treatments for corneal defects are topical and consist of the application of eyedrops. Unfortunately, three aspects make this strategy inappropriate for numerous pathologies. First, the frequent lack of patient compliance with a prescribed eyedrop regimen tends to aggravate corneal defects.[11] Second, the use of eyedrops can lead to the bacterial contamination of the container.[55] Third, there is a lack of any topical treatment for some corneal defects. The use of LG as a bioreactor to produce therapeutical tears therefore shows promise. That said, a number of barriers to such use remain, such as the safety of different transgenes for the LG and the necessity of adapting the timing of targeted protein secretion to the pathological context. Finally, certain specific conditions may be incompatible with this approach, such as contexts in which the LG is defective.

Collectively, our results show that LG gene therapy could be established to modify specifically the tear film to support corneal physiology. The main challenge in using AAV vectors for epithelial organ gene therapy is the high renewal rate of epithelial cells. In this study, we demonstrate that there is a non-renewing cell population in the LG that retains the secretory capacity to produce a large amount of mNGF for a period of 6 months. The long-term oversecretion of mNGF could replace the use of NGF-supplemented eyedrops, which are currently used to treat the NK observed in diabetes[7] or neurodegenerative diseases,[56] for example. Notably, by substituting mNGF with another gene, other corneal defects could be treated.

MATERIALS AND METHODS

Study design

The goals of this study were to assess the transduction pattern of AAV vector serotypes 2/5 and 2/9 after a single injection into murine LG, and

then, to evaluate the efficiency and the safety of an AAV2/9-mediated gene transfer of mNGF in the murine LG, for its secretion in the tear film. The main readouts of this study included the transduction pattern analyzed by immunohistochemistry (IHC) and western blot, the secretion of mNGF measured in tears by ELISA and Western blot, the AAV2/9 biodistribution by qPCR, the injection biosafety by analyzing the corneal integrity and innervation, the volume of tears, and the protein concentration in tears. Experimental groups were sized according to the literature to allow statistical analysis. No outliers were excluded from the study, except mice exhibiting spontaneous eye damage after the surgery or during the experiments. Behavioral data obtained from animals displaying eye damage unrelated to the abrasion procedure during the study were excluded. Scientists who performed the experiments and analysis were blinded to the group's identity. Data were analyzed by those carrying out the experiments and verified by the supervisor.

Cloning and vector production

The recombinant AAV vectors developed are called AAV hereafter. Cloning of the enhanced GFP (EGFP) and the mNGF in pAAV and AAV vector productions were provided by the vector core of the TarGeT (Translational Gene Therapy) Laboratory of Nantes, INSERM UMR 1089 (Nantes University, France). Briefly, single-stranded AAV2/5 and AAV2/9 CAG-GFP, single-stranded AAV2/5 and AAV2/9 CAG-mNGF vectors were obtained from pAAV CAG-GFP and pAAV CAG-mNGF plasmids, respectively, containing AAV2 inverted terminal sequences, CAG promoter, and bovine growth hormone (BGH) polyA signal. AAV2/5 and AAV2/9 CAG-GFP vectors were used to assess the transduction pattern after injection in the murine LG. AAV2/5 and AAV2/9 CAG-mNGF vectors were used to evaluate the efficiency of an AAV-based gene transfer in the LG, allowing mNGF secretion in the tear fluid.

Vector production was performed following the protocol of vector core of the TarGeT Laboratory of Nantes.[57] Briefly, recombinant AAVs were manufactured by co-transfection of HEK293 cells and purified by cesium chloride density gradients followed by extensive dialysis against phosphate-buffered saline (PBS). This approach is the main reference methodology used to manufacture the rAVV8RSM (reference standard material).[58] Vector titers were determined by qPCR and expressed as vector genome per milliliter. The target amplicons correspond to the inverted terminal repeat (ITR) sequences ITR-2 (ITR-2 forward: GGAACCCCTAGTGATGGAGTT, ITR-2 reverse: CGGCCTCAGTGAGCGA, TaqMan probe used for vector titer: FAM- CACTCCCTCTCTGCGCGCTCG-BBQ). Vectors containing AAV2/5 and AAV2/9 empty capsid served as controls. These controls are directly derived from the production of the vectors AAV2/5 and AAV2/9 CAG-GFP, respectively. In particular, during the purification process, the empty capsid vector controls come from a specific fraction (empty capsid fraction) collected from the cesium chloride gradient.[59]

Animals included in this study

All of the mice experiments were approved by the local ethical committee and the Ministère de la Recherche et de l'enseignement Supérieur (authorization 2016080510211993 version2). All of the procedures were performed in accordance with the French regulation for the animal procedure (French decree 2013-118) and with specific European Union guidelines for the protection of animal welfare (Directive 2010/63/EU). Mice were maintained on a 12-h dark-12-h light cycle, with a relative humidity between 40% and 60% and an ambient temperature of 21°C–22°C.

Surgery and vector delivery

Twelve-week-old Swiss/CD1 female mice (Janvier Labs, France) were injected into the central aspect of the right extraorbital LG. The LG injection of AAV vectors was performed under anesthesia with a mixture of ketamine (70 mg/kg, Imalgene 1000, Centravet, France) and medetomidine (1 mg/kg, Domitor, Centravet, France). One drop of Ocry-gel (Centravet) was applied to each eye. The skin on the cheek under the right ear was disinfected with vetedine solution (Centravet) and ethanol 70% and then cut above the LG location. Next, the viral solution was injected using a 34G beveled needle (Hamilton, USA, reference 207434) linked to a 10-µL Hamilton syringe (1701 RN serie, Hamilton, reference 7653-01). Wounds were closed by suture wires (Novosyn 6/0, reference C0068006, B Braun, Germany) and then disinfected with vetedine solution (Centravet). After surgery, mice were treated with buprenorphine (100 µg/kg, Brupecare, Centravet) and were woken up with atipamezole (1 mg/kg, Antisedan, Centravet). The injection procedure is delicate and some training is beneficial to increase the reproducibility of the procedure.

AAV vector solutions were prepared by diluting vectors at the right titer with sterile PBS and 0.01% of Fast Green (Sigma-Aldrich, USA, reference F7252). For all of the experimental studies, mice were unilaterally injected in the right extraorbital LG with 3 µL of vectors indicated below. For the transduction pattern study, AAV2/5 and AAV2/9 CAG GFP were injected at 10^{10} VG/LG (n = 6 mice per group, 3 for IHC analysis and 3 for western blot analysis). For the dose-response study, AAV2/9 CAG-mNGF was injected at 10^{9}, 10^{10}, or 10^{11} VG/LG (n = 5 mice per dose). For the kinetic study, AAV2/5 CAG-mNGF was injected at 10^{10} VG/LG and AAV2/9 CAG-mNGF was injected at 10^{10} and 10^{11} VG/LG (n = 5 mice per dose and per vector except at 240 Day Post Injection [DPI] n = 4 mice). For the biodistribution study, AAV2/9 CAG-mNGF was injected at 10^{11} VG/LG (n = 7 mice). For the biosafety study, AAV2/9 CAG-mNGF was injected at 10^{11} VG/LG (n = 5 mice for the tear volume and protein concentration analysis except at 240 DPI n = 4 mice, n = 3 mice for the corneal innervation study, n = 5 mice for the corneal sensitivity analysis). Animals injected with AAV2/5 or AAV2/9 empty capsid served as control (n = 3–7 mice as indicated in the figure legends).

Corneal abrasion

Corneal abrasions were performed as previously described.[1,3,60] Briefly, an ocular burr (Algerbrush II, reference BR2-5 0.5 mm, The Alger Company, USA) was used on mice that were anesthetized with a mixture of ketamine (70 mg/kg, Imalgene 1000) and medetomidine (1 mg/kg). Abrasions were performed unilaterally. A

fluorescein solution (1% in PBS, Sigma-Aldrich) was used to visualize the wound under a cobalt blue light. After abrasion, one drop of Ocrygel was applied to each eye; mice were treated with buprenorphine (100 μg/kg) and were woken up with atipamezole (1 mg/kg).

Tissue collection and processing

Tears were collected using a 1-μL microcapillary (Sigma-Aldrich, reference P1424) for 1 minute, 1 day before injection and 30 days post-injection for the dose-response and biodistribution studies; 1 day before injection and 7, 30, 60, 120, 180, and 240 days post-injection for the kinetic and biosafety studies; 1 day before abrasion and 1, 3, and 7 days post-abrasion for the corneal abrasion study.

For the transduction pattern and the biodistribution studies, mice were euthanized 30 days post-injection using pentobarbital (54.7 mg/mL, 140 mg/kg, Centravet). They were transcardially perfused with sterile PBS and tissues were quickly dissected. Tissues were then fixed for 45 min in 4% paraformaldehyde solution (AntigenFix, reference P0014, Diapath, France) at room temperature or directly snap-frozen in liquid nitrogen and stored at −80°C for IHC and molecular/biochemical analysis, respectively.

For whole-cornea imaging, mice were euthanized by cervical dislocation and enucleated with curved scissors by cutting the optic nerve. Collected eyes were then fixed for 20 min in 4% paraformaldehyde solution (AntigenFix) at room temperature. After PBS washes, eyes were dehydrated for 2 h in 50% ethanol/PBS and then stored at 4°C in 70% ethanol/PBS.

Tear volume, protein concentration, and mNGF analyses in tears

The volume of tears per minute (in microliters per minute) and the protein concentration in tears (in milligrams per milliliter) using the BCA protein assay kit (Fisher Scientific, France, reference 10678484) were measured and expressed as the mean ± SD.

The mNGF level in tears upon an AAV2/9 CAG-mNGF injection in the LG was dosed using the mNGF ELISA kit (Sigma-Aldrich, reference RAB1119) following the manufacturer's recommendations. Measures were performed on a CLARIOstar microplate reader (BMG Labtech, France) and analyzed using the CLARIOstar software (version 5.60 R2). Results are expressed as the mean ± SD.

IHC study

The following antibodies were used for IHC studies: chicken anti-GFP (Aves Labs, reference GFP-1020, 1/1,000), mouse anti-Ecadh (BD Biosciences, USA, reference 610182, 1/300), rabbit anti-Krt19 (Abcam, UK, reference ab52625, 1/200), rabbit anti-βIII tubulin (Abcam, reference ab18207, 1/1,000), goat anti-chicken Alexa Fluor 488 (Thermo Fisher Scientific, USA, reference A-32931, 1/500), goat anti-mouse Alexa Fluor 568 (Thermo Fisher Scientific, reference A-11004, 1/500), goat anti-rabbit Alexa Fluor 568 (Abcam, reference ab175471, 1/500), goat anti-rabbit Alexa Fluor 488 (Abcam, reference ab11008, 1/500), and goat anti-rabbit Alexa Fluor 568 (Abcam, reference ab175471, 1/500). Nuclei were counterstained with Hoechst 33342 (Thermo Fisher Scientific, reference H3570, 1/2,000) and BioTracker NIR694 (Merck, USA, reference SCT118, 1/400).

IHC on LG frozen sections

Following fixation, LG were incubated for 24 h in 2 successive baths of 6% and 30% sucrose and then embedded in optimal cutting temperature (OCT tissue freezing medium, MM France, reference F/TFM-C) and stored at −80°C. Longitudinal sections (10 μm thickness) were cut using a cryostat apparatus (LEICA CM3050, Leica Biosystems, USA). For primary antibodies produced in rabbits and chickens, cryosections were blocked with a mixture of 5% goat serum (GS, Thermo Fisher Scientific, reference 16210064), 5% of fish skin gelatin (FSG, Sigma-Aldrich, reference G7765), and 0.1% Triton X-100 in PBS for 1 h at room temperature. For primary antibodies produced in mouse (mouse anti-Ecadh), the blocking step described above was followed by an incubation with goat anti-mouse immunoglobulins (Abcam, reference ab6668, 1/200) for 1 h at room temperature. Cryosections were then incubated overnight at 4°C with primary antibodies diluted in GS/FSG/Triton/PBS mixture, washed 3 times with 0.1% Triton X-100/PBS, and subsequently incubated 1 h at room temperature with secondary antibodies diluted in GS/FSG/Triton/PBS mixture. After several PBS washes, cryosections were mounted in Fluoromount-G mounting medium (Invitrogen, USA, reference 00-4958-02).

IHC on whole cornea

Eyes were rehydrated in 50% ethanol/PBS during 2 h and washed twice in PBS for 15 min at room temperature. Corneas were dissected and permeabilized with 0.5% Triton X-100/PBS on a rocking agitator for 1 h and then blocked in 5% GS (Thermo Fisher Scientific, reference 16210064) and 2.5% FSG (Sigma-Aldrich, reference G7765) in 0.1% Triton X-100/PBS at room temperature. Corneas were incubated in primary antibody diluted in blocking solution overnight at 4°C on a rocking agitator and rinsed in 0.1% Triton X-100/PBS at room temperature (3 times for 1 h). Next, samples were incubated with secondary antibodies as previously mentioned. After the washes, nuclei were stained 10 min with BioTracker NIR694 (Merck, reference SCT118) and washed in PBS. Corneas were cut at four corners and mounted in Fluoromount-G mounting medium (Invitrogen, reference 00-4958-02), with the epithelium facing the coverslip.

Imaging

LG images were acquired using Zen Black software (version 2.3 SP1, Zeiss, France) on an LSM 880 confocal microscope (Zeiss, France). Whole LG section images were obtained using a 20×/0.8 objective while co-immunostaining of GFP with E-cadh or Krt19 proteins were observed via 0.36-μm step size z stacks using a 63×/1.4 oil immersion objective. Images were then processed with Zen Black software (version 2.3 SP1, Zeiss) and Zen Blue lite software (version 3.2, Zeiss). Whole-cornea images were acquired using the navigator module on a Leica Thunder Imager Tissue microscope with the large volume computational clearing (LVCC) process. Images were obtained using a 20×/0.55 objective with LAS X software (3.7.4) and processed with Imaris Bitplane software (version 9.8.0). All of the

images from a single panel were acquired and processed with the same parameters.

Western blot

Frozen LGs were crushed with a pestle and mortar pre-cooled at −80°C, solubilized in Pierce RIPA lysis buffer (Thermo Fisher Scientific, reference 89900) supplemented with protease inhibitors (Halt Protease Inhibitor Cocktail, Thermo Fisher Scientific, reference 87786), homogenized on a rotating wheel at 4°C overnight, and then centrifuged at 16,900 × *g* (Centrifuge 5418R, Eppendorf, Germany) for 30 min at 4°C. Supernatants were recovered and protein concentration of LG lysates or collected tears were quantified using the BCA protein assay kit (Thermo Fisher Scientific, reference 10678484). Forty and 8 μg proteins from LG lysates and collected tears, respectively, were loaded on any kD precast polyacrylamide gels (Mini-Protean TGX gels, Bio-Rad, USA, reference 4568124). Proteins were transferred to nitrocellulose membranes (Trans-Blot Turbo Mini 0.2 μm Nitrocellulose Transfer Pack, Bio-Rad, reference 1704158) through a semi-dry transfer process (Bio-Rad Trans-Blot Turbo system). Membranes were incubated with the REVERT total protein stain solution (LI-COR Biosciences, France, reference 926-11015) to record the overall amount of protein per well. They were then blocked for 1 h at room temperature using Intercept blocking buffer (LI-COR Biosciences, reference 927-60001). They were incubated with the following primary antibodies overnight at 4°C in LI-COR blocking buffer: chicken anti-GFP (Aves Labs, reference GFP-1020, 1/2,000) or rabbit mNGF (Abcam, reference Ab52918, 1/500). Following 3 washes with Tris-buffered saline (TBS) containing 0.1% Tween (TBST) for 15 min, secondary antibodies were incubated at a 1/15,000 dilution in LI-COR blocking buffer: donkey anti-chicken IR Dye 800CW (LI-COR Biosciences, reference 926-32218) or donkey anti-rabbit IR Dye 800CW (LI-COR Biosciences, reference 926-32213). After 3 washes in TBST for 15 min, images were acquired with an Odyssey CLX LI-COR Imaging System, and the quantifications were performed with Image Studio lite software (version 5.2). The GFP and the mNGF protein levels were both normalized to the total amount of protein loaded per well. The results are expressed as the mean ± SD.

AAV2/9 biodistribution study

LG, liver, and heart from AAV2/9-CAG-mNGF-injected mice (1011 VG/LG, n = 7) were collected 1 month post-injection in DNA-free, RNAse/DNAse-free, and PCR inhibitor-free certified microtubes. Tissue samples were collected immediately after sacrifice, snap-frozen in liquid nitrogen, and stored at −80°C in conditions that minimize cross-contamination and avoid qPCR inhibition. Extraction of genomic DNA (gDNA) from tissues using the Gentra Puregene kit (Qiagen, France, reference 158445) and Tissue Lyser II (Qiagen, reference 85300) was performed in accordance with the manufacturer's recommendations. The VG copy number was determined using a primer/FAM-TAMRA probe combination designed to amplify a specific region of the *BGH* transgene (*BGH* forward: TCTAGTTGC CAGCCATCTGTTGT, *BGH* reverse: TGGGAGTGGCACCTTCCA, *BGH* probe: FAM-TCCCCCGTGCCTTCCTTGACC-TAMRA). qPCR analyses were conducted on a StepOne Plus apparatus (Applied Biosystems, USA, Thermo Fisher Scientific) using 50 ng gDNA in triplicate and the following cycling conditions: denaturation step (20 s, 95°C) followed by a total of 45 cycles (1 s, 95°C; 20 s, 60°C). All of the reactions were performed in a final volume of 20 μL containing template DNA, Premix Ex Taq (Takara/Ozyme, France, reference RR390L), 0.4 μL ROX reference dye (Takara/Ozyme, reference RR390L), 0.2 μmol/L of each primer and 0.1 μmol/L of TaqMan probe (dual-labeled probes, Sigma-Aldrich). Endogenous gDNA copy numbers were determined using the primers/FAM-BHQ1 probe combination, designed to amplify a specific region of the murine *Albumin* sequence (murine *Albumin* forward: AACTGAAACTTTGGG AGGT, murine *Albumin* reverse: GGAGCACTTCATTCTCTGAC, murine *Albumin* probe: FAM-AGCTTGATGGTGTGAAGGAGAA AG-BHQ1). qPCR analyses were conducted on a C1000 touch thermal cycler (Bio-Rad) using 50 ng gDNA in triplicate and the following cycling conditions: denaturation step (20 s, 95°C), followed by a total of 45 cycles (3 s, 95°C; 30 s, 60°C). All of the reactions were performed in a final volume of 20 μL containing template DNA, Premix Ex Taq (Takara/Ozyme, reference RR390L), 0.25 μmol/L of each primer and 0.2 μmol/L of TaqMan probe (dual-labeled probes, Sigma-Aldrich). For each sample, threshold cycle (Ct) values were compared with those obtained with different dilutions of linearized standard plasmids (containing either the *BGH* expression cassette or the murine *Albumin* gene) using Bio-Rad CFX Maestro 2.2 software (version 5.2.008.0222) or StepOne software (version 2.3) for the C1000 touch thermal cycler and the StepOne Plus apparatus, respectively. The absence of qPCR inhibition in the presence of gDNA was checked by analyzing 50 ng gDNA extracted from tissue samples from 2 AAV2/9 empty capsid-injected control mice. Results were expressed in VG copies per DG as the mean ± SD. The lowest limit of quantification (LLOQ) was determined as 0.001 VG/DG. Only values of vector genome per diploid genome above the LLOQ were presented.

von Frey test

Corneal sensitivity was evaluated using von Frey filaments (Bioseb, France, reference bio-VF-M), as previously described.[61] Filaments with defined forces from 0.008 to 0.6 g were applied on the cornea of an immobilized mouse until an eye-blink reflex was observed. Mice were habituated every day for 5 days. The von Frey test was performed on each cornea for 2 consecutive days (contralateral side and injected side). The values obtained from these 2 days were averaged for each cornea. As the values were represented in grams, we displayed them as 1/g to reflect the sensitivity. Results are expressed as the mean ± SD. Behavioral experiments and analysis were performed by the same experimenter in single-blinded conditions throughout the study.

Statistical analysis

Data were analyzed with GraphPad Prism software (version 9.1.2, GraphPad, USA) and expressed as the mean ± SD, as indicated in the figure legends. Statistical differences between mean values were tested using Brown-Forsythe and Welch ANOVA tests followed by Dunnett's T3 multiple comparisons test, mixed-effects analysis

followed by Sidak's multiple comparisons test, mixed-effects analysis followed by Holm-Sidak's multiple comparisons test, repeated measure one-way ANOVA test followed by Dunnett's comparisons test, two-way ANOVA test followed by Sidak's multiple comparisons test, repeated-measures two-way ANOVA test followed by Tukey's comparisons test, or simple linear regression as indicated in the figure legends. Differences between values were considered significant with $^{*}p < 0.05$, $^{**}p < 0.01$, $^{***}p < 0.001$, and $^{****}p < 0.0001$.

DATA AND MATERIALS AVAILABILITY

All of the data and materials are available upon request.

SUPPLEMENTAL INFORMATION

Supplemental information can be found online at https://doi.org/10.1016/j.omtm.2022.08.006.

ACKNOWLEDGMENTS

The authors thank the different technical platforms of the Institute for Neurosciences of Montpellier, especially the RAM-Neuro, animal core facility supervised by Denis Greuet, the imaging facility MRI, member of the France Bio-Imaging national infrastructure supported by the French National Research Agency (ANR-10-INBS-04, "Investments for the Future'), and the CPV vector core and Preclinical Analytics Core from the TarGeT lab, INSERM UMR 1089, Nantes University (https://umr1089.univ-nantes.fr/facilities-cores/). This research was supported by the ATIP-Avenir program, Inserm Transfert, Inserm, Région Occitanie, University of Montpellier, French National Research Agency (ANR-21-CE17-0061), Groupama Foundation, and Retina France. The graphical abstract was created using BioRender.com.

AUTHOR CONTRIBUTIONS

Conceptualization, B.G. and F.M.; methodology, B.G., L.M., and L.H.; validation, B.G. and F.M.; formal analysis, B.G., L.H., and F.M.; investigation, B.G., L.M., C.A., L.H., N.F., A.K., A.B., C.L., V.B., and F.M.; data analysis, B.G. and F.M.; writing – original draft, B.G. and F.M.; writing – review & editing, all of the authors; supervision, F.M.; project administration, F.M.; funding acquisition, C.D. and F.M.

DECLARATION OF INTERESTS

The authors declare no competing interests.

REFERENCES

1. Kalha, S., Shrestha, B., Sanz Navarro, M., Jones, K.B., Klein, O.D., and Michon, F. (2018). Bmi1+ progenitor cell dynamics in murine cornea during homeostasis and wound healing. Stem Cell. *36*, 562–573.
2. Zieske, J.D. (2004). Corneal development associated with eyelid opening. Int. J. Dev. Biol. *48*, 903–911.
3. Kuony, A., Ikkala, K., Kalha, S., Magalhães, A.C., Pirttiniemi, A., and Michon, F. (2019). Ectodysplasin-A signaling is a key integrator in the lacrimal gland–cornea feedback loop. Development *146*. dev176693.
4. Lambiase, A., and Sacchetti, M. (2014). Diagnosis and management of neurotrophic keratitis. Clin. Ophthalmol. *8*, 571–579.
5. Müller, L.J., Marfurt, C.F., Kruse, F., and Tervo, T.M.T. (2003). Corneal nerves: structure, contents and function. Exp. Eye Res. *76*, 521–542.
6. Mastropasqua, L., Massaro-Giordano, G., Nubile, M., and Sacchetti, M. (2017). Understanding the pathogenesis of neurotrophic keratitis: the role of corneal nerves: the role of corneal nerves in neurotrophic keratitis. J. Cell. Physiol. *232*, 717–724.
7. Markoulli, M., Flanagan, J., Tummanapalli, S.S., Wu, J., and Willcox, M. (2018). The impact of diabetes on corneal nerve morphology and ocular surface integrity. Ocul. Surf. *16*, 45–57.
8. Han, S.B., Yang, H.K., and Hyon, J.Y. (2019). Influence of diabetes mellitus on anterior segment of the eye. Clin. Interv. Aging *14*, 53–63.
9. Yeh, S.-I., Chu, T.-W., Cheng, H.-C., Wu, C.-H., and Tsao, Y.-P. (2020). The use of autologous serum to reverse severe contact lens-induced limbal stem cell deficiency. Cornea *39*, 736–741.
10. Kanu, L.N., and Ciolino, J.B. (2021). Nerve growth factor as an ocular therapy: applications, challenges, and future directions. Semin. Ophthalmol. *36*, 224–231.
11. Eaton, A.M., Gordon, G.M., Konowal, A., Allen, A., Allen, M., Sgarlata, A., Gao, G., Wafapoor, H., and Avery, R.L. (2015). A novel eye drop application monitor to assess patient compliance with a prescribed regimen: a pilot study. Eye *29*, 1383–1391.
12. Wang, D., Tai, P.W.L., and Gao, G. (2019). Adeno-associated virus vector as a platform for gene therapy delivery. Nat. Rev. Drug Discov. *18*, 358–378.
13. Mendell, J.R., Al-Zaidy, S.A., Rodino-Klapac, L.R., Goodspeed, K., Gray, S.J., Kay, C.N., Boye, S.L., Boye, S.E., George, L.A., Salabarria, S., et al. (2021). Current clinical applications of in vivo gene therapy with AAVs. Mol. Ther. *29*, 464–488.
14. Kuzmin, D.A., Shutova, M.V., Johnston, N.R., Smith, O.P., Fedorin, V.V., Kukushkin, Y.S., van der Loo, J.C.M., and Johnstone, E.C. (2021). The clinical landscape for AAV gene therapies. Nat. Rev. Drug Discov. *20*, 173–174.
15. Maguire, A.M., Russell, S., Chung, D.C., Yu, Z.-F., Tillman, A., Drack, A.V., Simonelli, F., Leroy, B.P., Reape, K.Z., High, K.A., and Bennett, J. (2021). Durability of voretigene neparvovec for biallelic RPE65-mediated inherited retinal disease: phase 3 results at 3 and 4 years. Ophthalmology *128*, 1460–1468.
16. Day, J.W., Finkel, R.S., Chiriboga, C.A., Connolly, A.M., Crawford, T.O., Darras, B.T., Iannaccone, S.T., Kuntz, N.L., Peña, L.D.M., Shieh, P.B., et al. (2021). Onasemnogene abeparvovec gene therapy for symptomatic infantile-onset spinal muscular atrophy in patients with two copies of SMN2 (STR1VE): an open-label, single-arm, multicentre, phase 3 trial. Lancet Neurol. *20*, 284–293.
17. Auricchio, A., Smith, A.J., and Ali, R.R. (2017). The future looks brighter after 25 Years of retinal gene therapy. Hum. Gene Ther. *28*, 982–987.
18. Mohan, R.R., Martin, L.M., and Sinha, N.R. (2021). Novel insights into gene therapy in the cornea. Exp. Eye Res. *202*, 108361.
19. Rocha, E.M., Di Pasquale, G., Riveros, P.P., Quinn, K., Handelman, B., and Chiorini, J.A. (2011). Transduction, tropism, and biodistribution of AAV vectors in the lacrimal gland. Invest. Ophthalmol. Vis. Sci. *52*, 9567–9572.
20. Thomas, P.B., Samant, D.M., Selvam, S., Wei, R.H., Wang, Y., Stevenson, D., Schechter, J.E., Apparailly, F., Mircheff, A.K., and Trousdale, M.D. (2010). Adeno-associated virus-mediated IL-10 gene transfer suppresses lacrimal gland immunopathology in a rabbit model of autoimmune dacryoadenitis. Invest. Ophthalmol. Vis. Sci. *51*, 5137–5144.
21. Klenkler, B., Sheardown, H., and Jones, L. (2007). Growth factors in the tear film: role in tissue maintenance, wound healing, and ocular pathology. Ocul. Surf. *5*, 228–239.
22. Deeks, E.D., and Lamb, Y.N. (2020). Cenegermin: a review in neurotrophic keratitis. Drugs *80*, 489–494.
23. Kuony, A., and Michon, F. (2017). Epithelial markers aSMA, Krt14, and Krt19 unveil elements of murine lacrimal gland morphogenesis and maturation. Front. Physiol. *8*, 739.
24. Bax, B., Blundell, T.L., Murray-Rust, J., and McDonald, N.Q. (1997). Structure of mouse 7S NGF: a complex of nerve growth factor with four binding proteins. Structure *5*, 1275–1285.
25. Yan, R., Yalinca, H., Paoletti, F., Gobbo, F., Marchetti, L., Kuzmanic, A., Lamba, D., Gervasio, F.L., Konarev, P.V., Cattaneo, A., and Pastore, A. (2019). The structure of the pro-domain of mouse proNGF in contact with the NGF domain. Structure *27*, 78–89.e3.
26. Bonini, S., Aloe, L., Bonini, S., Rama, P., Lamagna, A., and Lambiase, A. (2002). Nerve growth factor (NGF): an important molecule for trophism and healing of the ocular surface. Adv. Exp. Med. Biol. *506*, 531–537.

27. de Souza, R.G., de Paiva, C.S., and Alves, M.R. (2019). Age-related autoimmune changes in lacrimal glands. Immune Netw. *19*, e3.

28. Guier, C.P., and Stokkermans, T.J. (2022). Cornea foreign body removal. In StatPearls (StatPearls Publishing).

29. Barrientez, B., Nicholas, S.E., Whelchel, A., Sharif, R., Hjortdal, J., and Karamichos, D. (2019). Corneal injury: clinical and molecular aspects. Exp. Eye Res. *186*, 107709.

30. Craig, J.P., Nichols, K.K., Akpek, E.K., Caffery, B., Dua, H.S., Joo, C.-K., Liu, Z., Nelson, J.D., Nichols, J.J., Tsubota, K., and Stapleton, F. (2017). TFOS DEWS II definition and classification report. Ocul. Surf. *15*, 276–283.

31. Ogawa, Y., Takeuchi, T., and Tsubota, K. (2021). Autoimmune epithelitis and chronic inflammation in sjögren's syndrome-related dry eye disease. Int. J. Mol. Sci. *22*, 11820.

32. Inomata, T., Sung, J., Nakamura, M., Iwagami, M., Okumura, Y., Iwata, N., Midorikawa-Inomata, A., Fujimoto, K., Eguchi, A., Nagino, K., et al. (2020). Using medical big data to develop personalized medicine for dry eye disease. Cornea *39*, S39–S46.

33. Abdul-Al, M., Kyeremeh, G.K., Saeinasab, M., Heidari Keshel, S., and Sefat, F. (2021). Stem cell niche microenvironment: review. Bioengineering *8*, 108.

34. Hudry, E., and Vandenberghe, L.H. (2019). Therapeutic AAV gene transfer to the nervous system: a clinical reality. Neuron *101*, 839–862.

35. Bordet, T., and Behar-Cohen, F. (2019). Ocular gene therapies in clinical practice: viral vectors and nonviral alternatives. Drug Discov. Today *24*, 1685–1693.

36. Ochakovski, G.A., Bartz-Schmidt, K.U., and Fischer, M.D. (2017). Retinal gene therapy: surgical vector delivery in the translation to clinical trials. Front. Neurosci. *11*, 174.

37. Schuster, D.J., Belur, L.R., Riedl, M.S., Schnell, S.A., Podetz-Pedersen, K.M., Kitto, K.F., McIvor, R.S., Vulchanova, L., and Fairbanks, C.A. (2014). Biodistribution of adeno-associated virus serotype 9 (AAV9) vector after intrathecal and intravenous delivery in mouse. Front. Neuroanat. *8*, 42.

38. Colle, M.-A., Piguet, F., Bertrand, L., Raoul, S., Bieche, I., Dubreil, L., Sloothaak, D., Bouquet, C., Moullier, P., Aubourg, P., et al. (2010). Efficient intracerebral delivery of AAV5 vector encoding human ARSA in non-human primate. Hum. Mol. Genet. *19*, 147–158.

39. Gautier, B., Hajjar, H., Soares, S., Berthelot, J., Deck, M., Abbou, S., Campbell, G., Ceprian, M., Gonzalez, S., Fovet, C.-M., et al. (2021). AAV2/9-mediated silencing of PMP22 prevents the development of pathological features in a rat model of Charcot-Marie-Tooth disease 1 A. Nat. Commun. *12*, 2356.

40. Powell, S.K., Rivera-Soto, R., and Gray, S.J. (2015). Viral expression cassette elements to enhance transgene target specificity and expression in gene therapy. Discov. Med. *19*, 49–57.

41. Gray, S.J., Foti, S.B., Schwartz, J.W., Bachaboina, L., Taylor-Blake, B., Coleman, J., Ehlers, M.D., Zylka, M.J., McCown, T.J., and Samulski, R.J. (2011). Optimizing promoters for recombinant adeno-associated virus-mediated gene expression in the peripheral and central nervous system using self-complementary vectors. Hum. Gene Ther. *22*, 1143–1153.

42. Grimm, D., Streetz, K.L., Jopling, C.L., Storm, T.A., Pandey, K., Davis, C.R., Marion, P., Salazar, F., and Kay, M.A. (2006). Fatality in mice due to oversaturation of cellular microRNA/short hairpin RNA pathways. Nature *441*, 537–541.

43. Auricchio, A., Kobinger, G., Anand, V., Hildinger, M., O'Connor, E., Maguire, A.M., Wilson, J.M., and Bennett, J. (2001). Exchange of surface proteins impacts on viral vector cellular specificity and transduction characteristics: the retina as a model. Hum. Mol. Genet. *10*, 3075–3081.

44. Hinderer, C., Katz, N., Buza, E.L., Dyer, C., Goode, T., Bell, P., Richman, L.K., and Wilson, J.M. (2018). Severe toxicity in nonhuman primates and piglets following high-dose intravenous administration of an adeno-associated virus vector expressing human SMN. Hum. Gene Ther. *29*, 285–298.

45. Haimovich, G., Ecker, C.M., Dunagin, M.C., Eggan, E., Raj, A., Gerst, J.E., and Singer, R.H. (2017). Intercellular mRNA trafficking via membrane nanotube-like extensions in mammalian cells. Proc. Natl. Acad. Sci. USA *114*, E9873–E9882.

46. Flemming, J.P., Hill, B.L., Haque, M.W., Raad, J., Bonder, C.S., Harshyne, L.A., Rodeck, U., Luginbuhl, A., Wahl, J.K., Tsai, K.Y., et al. (2020). miRNA- and cytokine-associated extracellular vesicles mediate squamous cell carcinomas. J. Extracell. Vesicles *9*, 1790159.

47. Tendler, Y., and Panshin, A. (2020). Features of p53 protein distribution in the corneal epithelium and corneal tear film. Sci. Rep. *10*, 10051.

48. Zincarelli, C., Soltys, S., Rengo, G., and Rabinowitz, J.E. (2008). Analysis of AAV serotypes 1–9 mediated gene expression and tropism in mice after systemic injection. Mol. Ther. *16*, 1073–1080.

49. Bailey, R.M., Armao, D., Nagabhushan Kalburgi, S., and Gray, S.J. (2018). Development of intrathecal AAV9 gene therapy for giant axonal neuropathy. Mol. Ther. Methods Clin. Dev. *9*, 160–171.

50. Brown, B.D., Venneri, M.A., Zingale, A., Sergi Sergi, L., and Naldini, L. (2006). Endogenous microRNA regulation suppresses transgene expression in hematopoietic lineages and enables stable gene transfer. Nat. Med. *12*, 585–591.

51. Konno, A., Takada, K., Saegusa, J., and Takiguchi, M. (2003). Presence of B7-2+ dendritic cells and expression of Th1 cytokines in the early development of sialodacryoadenitis in the IqI/Jic mouse model of primary Sjörgren's syndrome. Autoimmunity *36*, 247–254.

52. Dhouailly, D. (2009). A new scenario for the evolutionary origin of hair, feather, and avian scales. J. Anat. *214*, 587–606.

53. Colella, P., Ronzitti, G., and Mingozzi, F. (2018). Emerging issues in AAV-mediated *in vivo* gene therapy. Mol. Ther. Methods Clin. Dev. *8*, 87–104.

54. Sacchetti, M., Lambiase, A., Schmidl, D., Schmetterer, L., Ferrari, M., Mantelli, F., Allegretti, M., and Garhoefer, G. (2020). Effect of recombinant human nerve growth factor eye drops in patients with dry eye: a phase IIa, open label, multiple-dose study. Br. J. Ophthalmol. *104*, 127–135.

55. da Costa, A.X., Yu, M.C.Z., de Freitas, D., Cristovam, P.C., LaMonica, L.C., dos Santos, V.R., and Gomes, J.A.P. (2020). Microbial cross-contamination in multidose eyedrops: the impact of instillation angle and bottle geometry. Transl. Vis. Sci. Technol. *9*, 7.

56. Manni, L., Rocco, M.L., Bianchi, P., Soligo, M., Guaragna, M., Barbaro, S.P., and Aloe, L. (2013). Nerve growth factor: basic studies and possible therapeutic applications. Growth Factors *31*, 115–122.

57. Ayuso, E., Mingozzi, F., and Bosch, F. (2010). Production, purification and characterization of adeno-associated vectors. Curr. Gene Ther. *10*, 423–436.

58. Ayuso, E., Blouin, V., Lock, M., McGorray, S., Leon, X., Alvira, M.R., Auricchio, A., Bucher, S., Chtarto, A., Clark, K.R., et al. (2014). Manufacturing and characterization of a recombinant adeno-associated virus type 8 reference standard. Hum. Gene Ther. *25*, 977–987.

59. Tran, N.T., Lecomte, E., Saleun, S., Namkung, S., Robin, C., Weber, K., Devine, E., Blouin, V., Adjali, O., Ayuso, E., et al. (2022). Human and insect cell-produced recombinant adeno-associated viruses show differences in genome heterogeneity. Hum. Gene Ther. *33*, 371–388.

60. Kalha, S., Kuony, A., and Michon, F. (2018). Corneal epithelial abrasion with ocular burr as a model for cornea wound healing. J. Vis. Exp.58071 https://doi.org/10.3791/58071.

61. Fakih, D., Zhao, Z., Nicolle, P., Reboussin, E., Joubert, F., Luzu, J., Labbé, A., Rostène, W., Baudouin, C., Mélik Parsadaniantz, S., and Réaux-Le Goazigo, A. (2019). Chronic dry eye induced corneal hypersensitivity, neuroinflammatory responses, and synaptic plasticity in the mouse trigeminal brainstem. J. Neuroinflammation *16*, 268.